

## FINITE ELEMENT ANALYSIS OF DYNAMIC BEHAVIOR OF SALIENT POLES SYNCHRONOUS MOTOR

Virgiliu FIREȚEANU\*, Petrică TARĂȘ\*

\* POLITEHNICA University of Bucharest/Faculty of Electrical Engineering/  
EPM\_NM Laboratory, Bucharest, Romania  
[firetean@amotion.pub.ro](mailto:firetean@amotion.pub.ro)

**Abstract** – This paper explores dynamic actions of synchronous motor with salient poles based on finite element models and solutions of step by step in time domain type.

The motor startup in no-load and in-load conditions, without current in the field winding or with short-circuited field winding are analyzed. The motor dynamics and transient at suddenly increase of the load torque, without and with current in the field winding is studied, and the reluctant torque is evaluated

**Keywords:** salient poles synchronous motor, finite element analysis.

### 1. INTRODUCTION

The variant with salient poles and electrical absorber is the best solution for the synchronous machine operation as synchronous motor. The differences between this variant and those with constant air gap concern generally the states when the rotor speed is different from the synchronism value. That is why, in this paper is defined finite element models and is analyzed simulation results for motor startup and for suddenly changes of loaded torque.

All defined models are couplings of field - circuit - motion type and the numerical solutions are of finite element type with respect to the spatial coordinates and of step-by-step type in time domain.

### 2. GEOMETRY, PHYSICAL PROPERTIES, CIRCUIT MODEL AND MOTION COUPLING

The object of the study is a 4 salient poles synchronous machine with rated power 3 kVA, for the network 3 x 127/220 V, 50 Hz. A particular winding is placed in the slots of the four poles of the rotor magnetic core. This winding actions as a squirrel cage in case of asynchronous startup and as an electrical absorber in case of machine operation as synchronous motor or generator.

The 2D geometry of the computation domain, Fig. 1, represents half of the machine transversal section. It is not possible to reduce further more the computation domain to a quarter of transversal

section, since the number of stator slots is not divisible with 4.

Around the two rotor poles in the computation domain, Fig. 2, are placed the go-sides E1PLUS, E2PLUS and the return-sides E1MINUS, E2MINUS of the two coils of field winding.

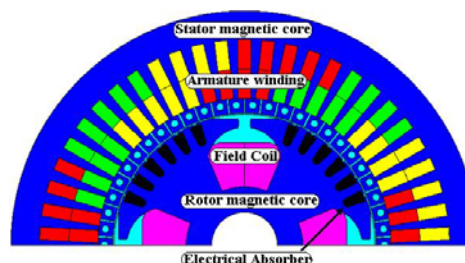


Figure 1. The computation domain

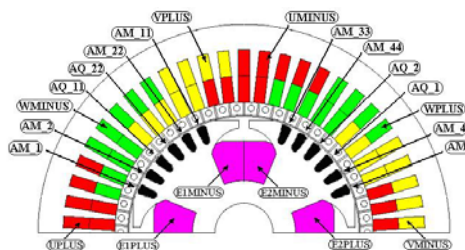


Figure 2. The winding type regions of the computation domain

The stator double layer winding has shortened coils opening and  $4\frac{1}{2}$  coils per pole and phase. The go- and respectively the return- coil sides of the three phases U, V and W of this winding are denominated UPLUS, VPLUS, WPLUS and respectively UMINUS, VMINUS, WMINUS.

The regions corresponding to the electrical absorber on the rotor, Fig. 2, are the bars AM\_1, AM\_2, AM\_11, AM\_22, AM\_3, AM\_4, AM\_33, AM\_44, AQ\_1, AQ\_2, AQ\_11, AQ\_22.

All the other faces of the computation domain are included in the nonconductive and nonmagnetic regions called AIR\_STAT and AIR\_ROT.

The computation domain, Fig. 1, is bound by the external contour of the stator magnetic core, the

internal contour of the rotor magnetic core and two radial line segments. The boundary conditions suppose null local value of the magnetic flux on the two round contours and a cyclic periodicity condition on the two radial lines. The last condition is valid when the computation domain contains an even number of poles.

The rotor and stator laminations are of magnetic non-linear steel made, whose  $B(H)$  dependence is defined by the relative initial magnetic permeability and the magnetic flux density at saturation.

The coils of field winding - B\_ROTOR, Fig. 3, and of stator winding, B1, B2, B3, are of stranded conductor type; consequently, the material model associated to these regions is non-magnetic and non-conductive. The numbers of turns of each stator phase and of each field coil are input data.

The electrical absorber is aluminum made.

The field model of the machine is coupled with the circuit model in figure 3, where the components B1, B2 and B3 represent coils of stranded conductor type, placed in stator slots. The coils L1, L2 and L3 simulate the portions of the stator windings outside the slots. Similarly, the stranded coil component B\_ROTOR and the coil L4 correspond to the field winding, inside, respectively outside the rotor magnetic core.

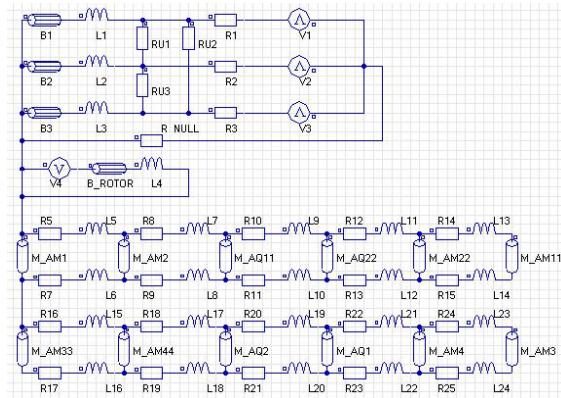


Figure 3. The circuit model of the studied machine

The voltage supply of field winding is V4, Fig. 3.

The part of electrical absorber inside the rotor magnetic core is implemented using components of solid conductor type - the bars M\_AM\_1, M\_AM\_2, M\_AM\_11, M\_AM\_22, M\_AM\_3, M\_AM\_4, M\_AM\_33, M\_AM\_44, M\_AQ\_1, M\_AQ\_2, M\_AQ\_11, M\_AQ\_22. The part of this absorber outside the rotor magnetic core, respectively the frontal short-circuit segment between bars are simulated by resistors and coils.

The electric resistance of resistors and of coils of stranded conductor type and the inductance of coils L1 ..., L24 are computation data, as well as the number of turns of stranded coil components B1, B2, B3 and B\_ROTOR.

The motor supply network is modeled by the voltage sources V1, V2 and V3 and their internal resistances R1, R2 and R3. The resistors RU1, RU2 and RU3 simulate voltmeters for phase-to-phase voltages evaluation.

A model of field - circuit - motion type in the study of electrical machines takes into account the equation the rotor dynamics:

$$J \frac{d\Omega}{dt} = M_e - M_r(\Omega) = M_e - (c_0 + c_1\Omega) \quad (1)$$

where  $J$  is the moment of inertia,  $M_e$  is the electromagnetic torque and  $M_r$  is the resistant torque. The quantity  $c_0$  represent the load torque and  $c_1\Omega$  is the friction torque.

The numerical solution of the field - circuit - motion coupling is obtained through the method called step by step in the time domain.

### 3. FINITE ELEMENT MODELS FOR THE STUDY OF SYNCHRONOUS MOTOR STARTUP

#### 3.1. No-load startup without field current

The startup of the studied salient poles synchronous motor is an asynchronous startup, since the electrical absorber winding operates as the squirrel cage of asynchronous motors. The study of the no-load asynchronous startup provides information on starting time, time variation of currents, electromagnetic torque and speed, value of steady state speed and current.

In the circuit model for the study of no-load startup dynamics a resistor with high resistance value replaces the voltage source V4, Fig. 3. This means the field winding terminals are connected to a voltmeter.

No-load torque is provided in the motion model, only a small value of friction torque is considered.

The instantaneous values of voltages of the three sources V1, V2 and V3, Fig. 3, are as follows:

$$\begin{aligned} u_1(t) &= 127\sqrt{2} \sin \omega t, u_2(t) = 127\sqrt{2} \sin(\omega t - 2\pi/3), \\ u_3(t) &= 127\sqrt{2} \sin(\omega t + 2\pi/3) \end{aligned} \quad (2)$$

As the curve speed - time in Figure 4 shows, the motor speed continuously increases during 1.2 s. After damped oscillations, the steady state speed that is the synchronous speed 1500 rpm is reached at 3 s. Further, the synchronous machine operates as a no-load synchronous motor, which means that the value of the reluctant torque due to the magnetic anisotropy of the rotor is greater than the friction torque. This component of the electromagnetic torque acting on the rotor is responsible with the synchronization of the machine at the end of asynchronous startup.

The time variation of the phase U stator current, of the current in the rotor bar AM\_1, Fig. 2, and of the

voltage induced in the field winding are presented in Figs 5, 6 and 7. Since the rated value of the stator current is  $3000/3/127 = 7.87$  A, the right curve in Figure 5, corresponding to the steady state no-load operation of the motor without field current, shows an over value of the stator current of 70 %. The high value of the field winding peak voltage during startup, around 1500 Volts, Fig. 7, affects the design of electric insulation scheme, whose DC rated supply voltage is only 10 Volts.

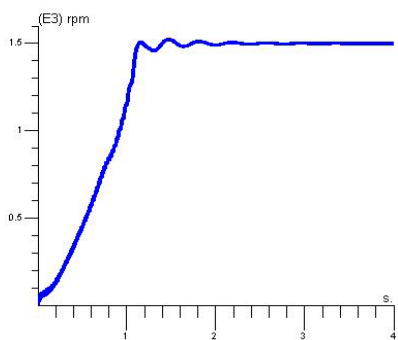


Figure 4. Speed variation during the no-load asynchronous startup

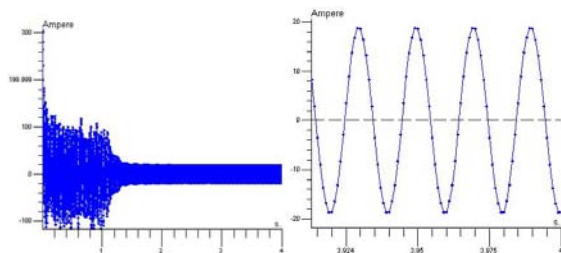


Figure 5. Time variation of the phase U stator current during the no-load startup

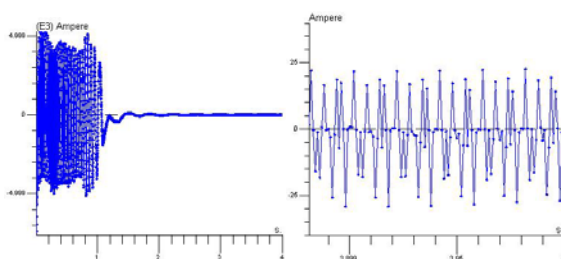


Figure 6. Time variation of the current in a rotor bar during the no-load startup

During the startup, the time variation of electromagnetic torque, Fig. 8, presents important oscillations around the mean value, which increases during the first second of startup. The result in figure 8 corresponds to the computation domain; consequently, the values of electromagnetic torque in this figure and in all similar ones are half of the actual values.

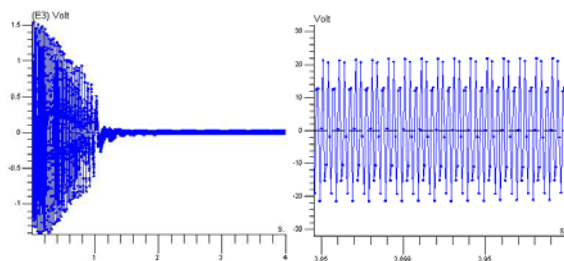


Figure 7. Time variation of the voltage induced in the field winding during the no-load startup

When steady state is reached, the mean value of the electromagnetic torque is close to zero.

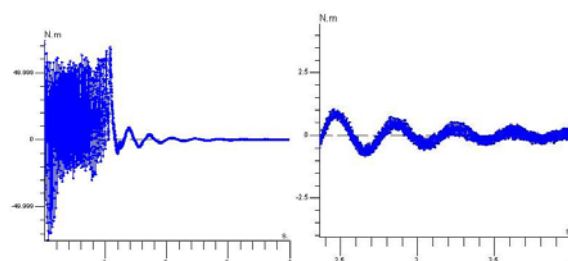


Figure 8. Time variation of electromagnetic torque during the no-load startup

### 3.2. Startup in-load without field current

It is interesting to see if the studied synchronous motor is able also to start in load, respectively when the resistive torque is not negligible. Consequently, this section answers to the question is it the reluctant torque of this machine with salient poles strong enough to pull the motor in synchronism when the resistive torque is 9.5 Nm. This torque corresponds to the value  $9.5 \times 2 \times \pi \times 1500/60 = 1492$  W of the motor output power. The time variation of the speed, Fig. 9, shows the answer is yes.

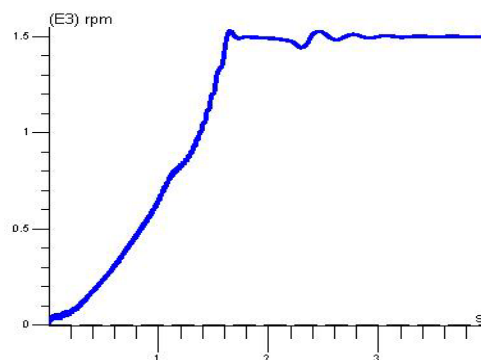


Figure 9. Time variation of speed during the startup in-load

As expected, the startup time, Figs. 10, 11 is longer than in case of no-load startup and the steady state stator current, Fig. 10, has an increased value.

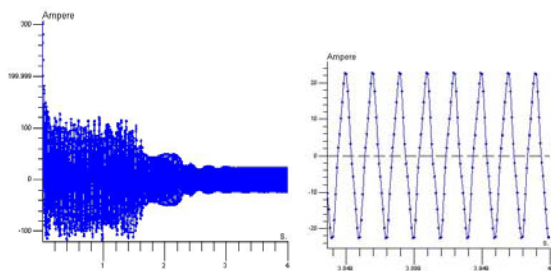


Figure 10. Time variation of stator current during the startup in-load

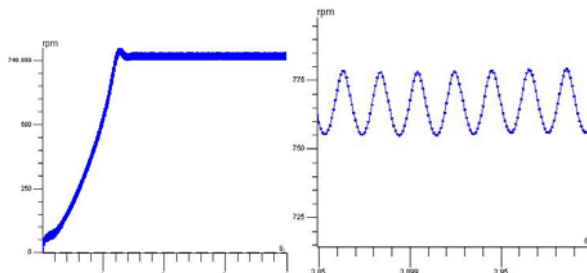


Fig. 13. Time variation of speed during the startup in load with short-circuited field winding

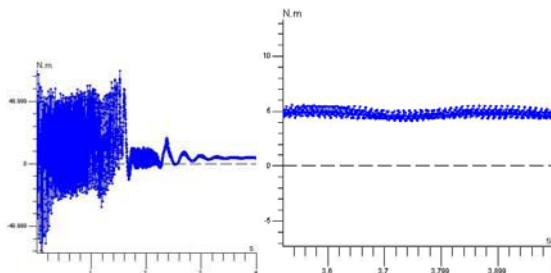


Figure 11. Time variation of electromagnetic torque during the startup in load

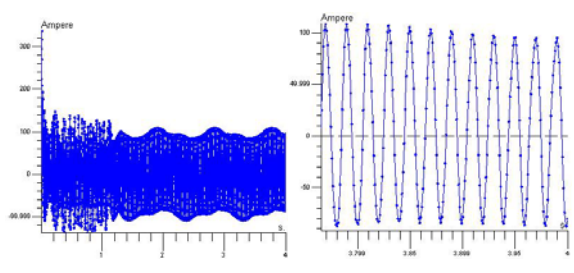


Figure 14. Time variation of stator current during the startup in load with short-circuited field winding

### 3.3. Startup in-load with short-circuited field winding (Georges phenomenon)

This startup model considers the field winding is short-circuited. The current induced in the field winding, Fig. 12, generates a heteropolar magnetic field, which is responsible for Georges phenomenon. This phenomenon explains why the steady state mean speed of motor is far from the synchronous speed, Fig. 13. As seen, the oscillations of the speed around the mean value are not negligible.

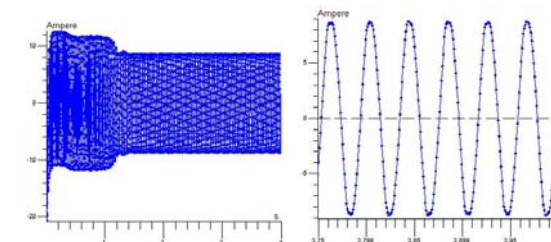


Figure 12. Time variation of current in the short-circuited field winding during the startup in-load

The steady state operation of the motor after the startup with short-circuited field winding is unacceptable because the stator current, Fig. 14, is much higher than the rated value.

### 3.4. Startup in-load with field winding connected on a resistor

Now, the field winding terminals are connected by a resistor whose resistance  $25 \Omega$  is chose so that the machine is still able to avoid the Georges phenomenon during the startup in-load.

During startup, the speed has the tendency to remain around 800 rpm, Fig. 15, but after 1.7 s the rotor accelerates again towards the synchronous speed. The voltage induced in the field winding, Fig. 16, is much smaller comparing the dangerous initial value evaluated in section 3.1.

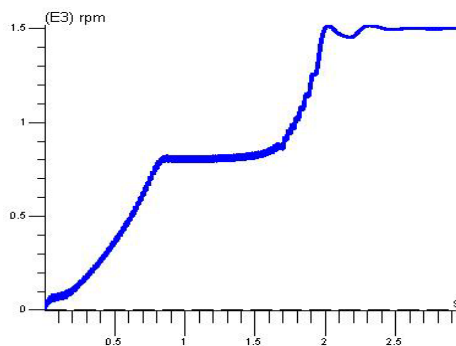


Figure 15. Time variation of speed during the startup in load with field winding connected on a resistor

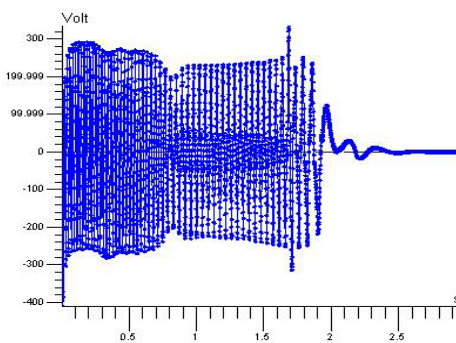


Figure 16. Field winding voltage during the startup in-load with field winding connected on a resistor

#### 4. DYNAMICS AND TRANSIENT WITHOUT FIELD CURRENT WHEN THE LOAD TORQUE SUDDENLY INCREASES

The finite element model in this section considers as initial state the final time step of the motor startup in-load (9.5 Nm) without current in the field winding. The load torque suddenly increases to 30 Nm, which corresponds to a power higher than the rated value.

Figure 17 shows periodically oscillations of the motor speed, between 1405 rpm and 1520 rpm. The motor has no the capability to maintain the synchronous speed. The stator current, Fig. 18, the time variation of the current in a rotor bar, Fig. 19, and of the electromagnetic torque, Fig. 20, show periodic tendency of the motor to reestablish the synchronism state, having the period 0.8 s.

Without field current the machine cannot properly operate at high loads. The rotor cage is not so efficient to insure the steady state operation as asynchronous motor, and the reluctant torque is not strong enough to synchronize the motor.

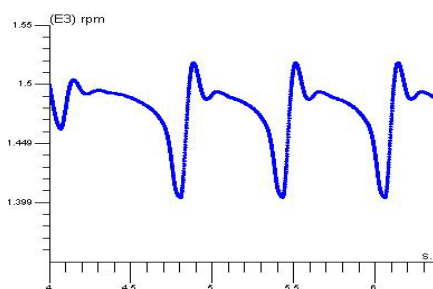


Figure 17. Time variation of rotor speed when the load torque suddenly increases

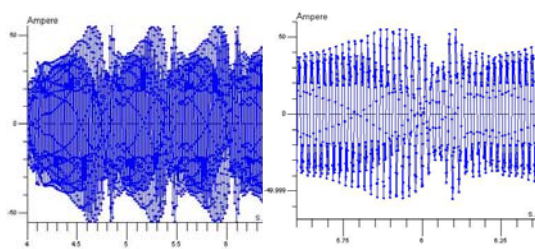


Figure 18. Time variation of stator current when the load torque suddenly increases

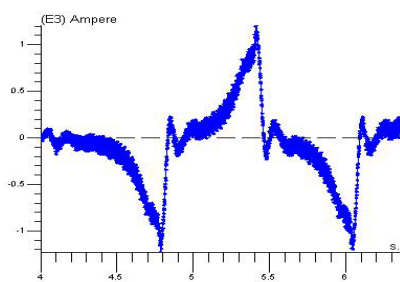


Figure 19. Time variation of the current in the rotor bar when the load torque suddenly increases

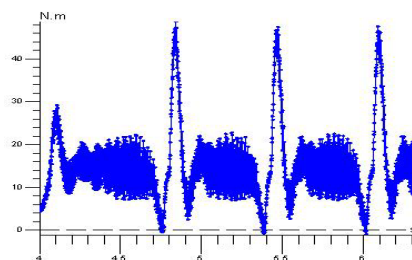


Figure 20. Time variation of the electromagnetic torque when the load torque suddenly increases

#### 5. DYNAMICS AND TRANSIENT WHEN THE LOAD TORQUE SUDDENLY INCREASES AND THE FIELD WINDING IS SUPPLIED

Previous results show that if the load is reduced comparatively to the rated load, the studied synchronous motor can start as an asynchronous motor and reach the synchronous speed without field current. But when the load is important, the motor cannot reach the synchronism.

The initial state of the model in this section corresponds to the final time step 4 s of the startup without field current and the load torque of 9.5 Nm. The load torque suddenly increases at 30 Nm and simultaneously the field winding is connected at a DC voltage source V4, Fig. 3, of 10 V.

In this case, as seen in Figure 21 after about 1 second of attenuated speed oscillations, the synchronism is reestablished. The time variations of the field current, of the stator current, of the current through a rotor bar and of the electromagnetic torque are presented in Figs. 22 – 25.

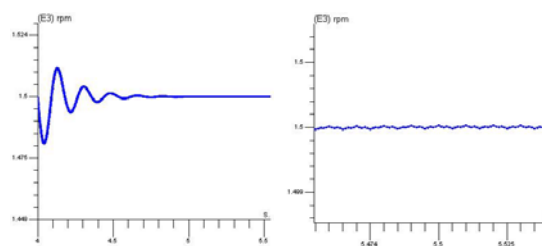


Figure 21. Time variation of speed when the load torque suddenly increases and simultaneously the field winding supply is connected

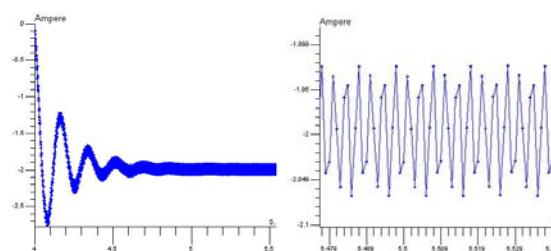


Figure 22. Time variation of field current when the load torque suddenly increases and simultaneously the field winding supply is connected

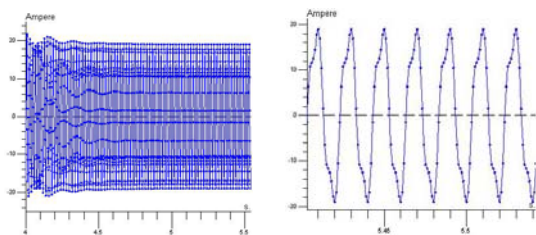


Figure 23. Time variation of stator current when the load torque suddenly increases and simultaneously the field winding supply is connected

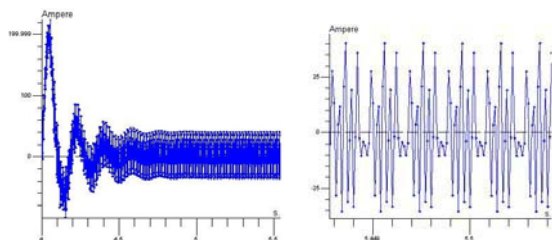


Figure 24. Time variation of current in a rotor bar when the load torque suddenly increases and simultaneously the field winding supply is connected

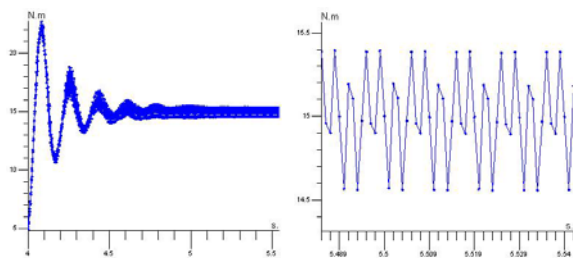


Figure 25. Time variation of electromagnetic torque when the load torque suddenly increases and simultaneously the field winding supply is connected

## 6. EVALUATION OF THE RELUCTANT TORQUE

As previously established, the reluctant torque is responsible for steady state no-load or reduced-load operation of the synchronous motor with salient poles at synchronous speed. The evaluation of this torque is investigated in this section, where the field winding and the electrical absorber winding are eliminated from the field model and from the circuit model. The only one source of the magnetic field rests the stator winding. Imposing a constant speed of the rotor equal with the synchronous speed, which is the rotation speed of the magnetic field, the electromagnetic torque acting on the rotor is the reluctant torque.

Figure 26 shows that after an electromagnetic transient of about 0.5 s the steady state corresponding to the right image is established. From this image it results the mean value  $1.44 \times 2 = 2.88$  Nm of the reluctant torque of the studied synchronous machine.

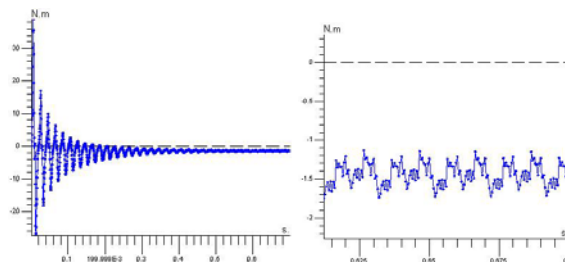


Figure 26. Time variation of the reluctant torque

## 7. CONCLUSIONS

The numerical experiments presented in this paper prove the efficiency of the studies of electrical machines based on finite element models. Relative complicated phenomena, like those characterizing the transient and dynamics of a synchronous motor with salient poles and electrical absorber are deeply analyzed using finite element models of the field - circuit - motion type.

The startup and steady state operation of the studied synchronous motor with salient poles based on the combined action of the electric absorber winding and of the reluctant torque is possible for no-load or relatively reduced-load conditions.

If during the startup the terminals of the field winding are free, the voltage induced in this winding is very high. On the other side, if the field winding is short-circuited the synchronous speed is not reached. Only connecting the terminals with a resistor of appropriate resistance value, these two drawbacks are eliminated.

It was proved that the studied synchronous motor is able to operate for important values of load, over the rated value, when, after the startup, the DC supply of the field winding is connected.

## References

- [1] S. J. Salon, *Finite Element Analysis of Electrical Machines*, Boston Kluwer Academic Publishers, 1995.
- [2] A. B. J. Reece and T. W. Preston, *Finite Element Method in Electrical Power Engineering*, Oxford University Press, 2000.
- [3] V. Fireșteanu, T. Tudorache and O. A. Țurcanu, "Optimal Design of Rotor Slots Geometry of Squirrel Cage Type Induction Motors", Proc. of IEMDC'07 Conference, Antalya, Turkey, 2007.
- [4] P. Taraș, V. Fireșteanu, "Teaching Synchronous Machines by Finite Element Models", Proc. of OPTIM'08 Conference, Brașov, Romania, 2008.